BJP BRITISH JOURNAL OF PHARMACOLOGY

BPS BRITISH PHARMACOLOGICAL SOCIETY

BJP British Journal of Pharmacology

DOI:10.1111/j.1476-5381.2010.00920.x
www.brjpharmacol.org

RESEARCH PAPER

Comparative pharmacology of chemically distinct NADPH oxidase inhibitors

S Wind[1], K Beuerlein[1], T Eucker[1], H Müller[1], P Scheurer[2], ME Armitage[3], H Ho[3], HHHW Schmidt[3,4] and K Wingler[3,4]

[1]*Rudolf-Buchheim-Institute for Pharmacology, Justus-Liebig-University, Gießen, Germany,* [2]*Vasopharm GmbH, Würzburg, Germany,* [3]*Florey Neuroscience Institutes, National Stroke Research Institute, Melbourne, Australia and* [4]*Department of Pharmacology and Toxicology, Cardiovascular Research Institute Maastricht, Maastricht University, The Netherlands*

Correspondence
Prof Harald Schmidt, Department of Pharmacology, Maastricht University, PO Box 616, 6200 MD Maastricht, The Netherlands.
E-mail:
h.schmidt@farmaco.unimaas.nl

Keywords
hypertension; NADPH oxidase; NOX; oxidative stress; reactive oxygen species

Received
20 October 2009
Revised
12 May 2010
Accepted
18 May 2010

BACKGROUND AND PURPOSE

Oxidative stress [i.e. increased levels of reactive oxygen species (ROS)] has been suggested as a pathomechanism of different diseases, although the disease-relevant sources of ROS remain to be identified. One of these sources may be NADPH oxidases. However, due to increasing concerns about the specificity of the compounds commonly used as NADPH oxidase inhibitors, data obtained with these compounds may have to be re-interpreted.

EXPERIMENTAL APPROACH

We compared the pharmacological profiles of the commonly used NADPH oxidase inhibitors, diphenylene iodonium (DPI), apocynin and 4-(2-amino-ethyl)-benzolsulphonyl-fluoride (AEBSF), as well as the novel triazolo pyrimidine VAS3947. We used several assays for detecting cellular and tissue ROS, as none of them is specific and artefact free.

KEY RESULTS

DPI abolished NADPH oxidase-mediated ROS formation, but also inhibited other flavo-enzymes such as NO synthase (NOS) and xanthine oxidase (XOD). Apocynin interfered with ROS detection and varied considerably in efficacy and potency, as did AEBSF. Conversely, the novel NADPH oxidase inhibitor, VAS3947, consistently inhibited NADPH oxidase activity in low micromolar concentrations, and interfered neither with ROS detection nor with XOD or eNOS activities. VAS3947 attenuated ROS formation in aortas of spontaneously hypertensive rats (SHRs), where NOS or XOD inhibitors were without effect.

CONCLUSIONS AND IMPLICATIONS

Our data suggest that triazolo pyrimidines such as VAS3947 are specific NADPH oxidase inhibitors, while DPI and apocynin can no longer be recommended. Based on the effects of VAS3947, NADPH oxidases appear to be a major source of ROS in aortas of SHRs.

Abbreviations

AEBSF, (4-2-amino-ethyl)-benzolsulphonyl-fluoride hydrochloride; AUC, area under the curve; CAT, catalase; COLDER, colour-developing reagent; DHE, dihydroethidium; DPI, diphenylene iodonium; eNOS, endothelial NOS; HBSS, Hanks's balanced salt solution; HUVEC, human umbilical vein endothelial cell; L-NAME, NG-nitro-L-arginine methyl ester; NOX, NADPH oxidase; OPZ, opsonized zymosan; oxLDL, oxidized LDL; PBS, phosphate-buffered saline; PMA, phorbol myristate acetate; ROS, reactive oxygen species; SHR, spontaneously hypertensive rat; SOD, superoxide dismutase; VSMC, vascular smooth muscle cell; WCH, whole-cell homogenate; WKY, Wistar Kyoto (rats); XOD, xanthine oxidase

Introduction

Growing evidence suggests that an overproduction of reactive oxygen species (ROS), such as superoxide, hydrogen peroxide, hydroxyl radicals and peroxynitrite, contributes to the pathogenesis of cardiovascular diseases (Stocker and Keaney, 2004). With respect to the relevant enzymatic sources of these ROS, the family of NADPH oxidases has received considerable attention (Griendling *et al.*, 2000; Cave *et al.*, 2006).

NADPH oxidases are comprised of membrane proteins (i.e. the catalytic flavin–heme protein); NOX, of which five isoforms exist (NOX1–5); and the non-catalytic 22 kDa binding protein, p22phox (Lassegue and Clempus, 2003). Other components of the NADPH oxidase complex can include a cytosolic organizer (p47phox or NOXO1), an activator (p67phox or NOXA1) and other proteins (p40phox and Rac). These cytosolic subunits vary with the different NOX isoforms (Opitz *et al.*, 2007). Upon phosphorylation, cytosolic subunits translocate to the NOX-containing membrane resulting in ROS formation. However, NOX4 and NOX5 may be independent of cytosolic subunits and constitutively active (Brandes and Kreuzer, 2005; Bedard and Krause, 2007; Lambeth *et al.*, 2007; Opitz *et al.*, 2007) or regulated by intracellular free calcium (Bedard and Krause, 2007) respectively.

The only known function of NADPH oxidases is to generate ROS. This feature makes NADPH oxidases distinct from other sources of ROS such as xanthine oxidase (XOD) or uncoupled NOS as these enzymes produce ROS only after conversion to a dysfunctional state. This is triggered by ROS derived from a primary source. NADPH oxidases may be this primary source of ROS, initiating oxidative stress and converting other enzymes into an ROS-producing state (McNally *et al.*, 2003) to eventually induce cardiovascular pathophysiology. To test this hypothesis, both genetic and pharmacological approaches have been pursued.

According to studies using genetically modified mice, NOX1 plays a role in the pathophysiology of hypertension (Matsuno *et al.*, 2005; Gavazzi *et al.*, 2006) and in neointima formation in mice (Lee *et al.*, 2009). However, pharmacological evidence – and thus the potential of translating these findings into therapeutic applications – has not yet been provided. This is mainly due to the lack of specific NADPH oxidase inhibitors. In particular, there are concerns about the specificity of compounds currently used as NADPH oxidase inhibitors. For example, one of the most frequently applied compounds, apocynin, may also act as an antioxidant (Heumuller *et al.*, 2008) and a Rho kinase inhibitor (Schluter *et al.*, 2008). Other compounds that have been widely used include 4-(2-aminoethyl)-benzenesulphonyl fluoride (AEBSF) (Bayraktutan, 2005), which blocks p47phox translocation to the membrane but also inhibits serine proteases (Diatchuk *et al.*, 1997), as well as diphenylene iodonium (DPI). DPI also inhibits other flavin-containing enzymes such as NOS and XOD (O'Donnell *et al.*, 1993), as well as cholinesterases and the internal calcium pump (Tazzeo *et al.*, 2009).

We here directly compared the specificity and efficacy of the most commonly investigated NADPH oxidase inhibitors in three different cell lines, and isolated enzyme preparations using several assays for ROS detection. We also analysed the compounds *in situ* in vascular tissue sections of spontaneously hypertensive rats (SHRs). We are aware that many, if not all, of the ROS assays have limitations with respect to specificity and artefacts (Dikalov *et al.*, 2007). Therefore, we followed current recommendations and used several of the most frequently used ROS detection systems in parallel to ensure that our data are not only representative, but also comparable to previous papers.

We included the triazolo pyrimidine VAS3947, a novel derivative of VAS2870 with higher solubility. VAS3947 has been developed by *in silico* optimization of VAS2870 (Tegtmeier *et al.*, 2005), which was recently shown to inhibit NADPH oxidase activity in primary rat vascular smooth muscle cells (VSMCs) (ten Freyhaus *et al.*, 2006), and human umbilical vein endothelial cells (HUVECs) (Stielow *et al.*, 2006). VAS2870 also inhibited wound margin H_2O_2 production without obvious toxicity in zebrafish larvae (Niethammer *et al.*, 2009), as well as platelet-derived growth factor (PDGF) BB-stimulated vasculogenesis of embryonic stem cell-derived endothelial cells (Lange *et al.*, 2009). We here show that, among the tested compounds, only VAS3947 was an apparently specific inhibitor of NADPH oxidases, which did not interfere with commonly used ROS assays. Using this novel inhibitor, we also provide pharmacological evidence that NADPH oxidases are indeed a relevant source of ROS in the SHR model of hypertension. Having established the specificity, future experiments are justified to determine the mechanism of action, the isoform specificity and the *in vivo* actions of this novel NADPH oxidase inhibitor compound class, which is beyond the scope of this study.

Methods

RNA isolation and RT-PCR

Total RNA was isolated from the human CaCo-2 and HL60, and the rat A7r5 cell lines using the RNeasy Kit (Qiagen, Hilden, Germany) and treated with

DNase I (Invitrogen, Karlsruhe, Germany) according to the manufacturers' protocols. Total RNA was then reverse transcribed by Superscript III using the protocol for random hexamer primers (Invitrogen). Thereafter, each reaction was treated with RNase H (Invitrogen) for 20 min at 37°C before PCR was performed [94°C 5 min, 94°C 1 min–60°C 1 min–72°C 30 s (35×), 72°C 10 min] using the following specific primers: human NOX1 (5′-tctctccagcctatctcatg-3′, 5′-ctcattcatgctctcctctg-3′), NOX2 (5′-tcctccaccaa aaccatccg-3′, 5′-aaaaccgcaccaacctctcac-3′), human NOX3 (5′-ctgccctgacagatgtatttc-3′, 5′-gtcagtattttcg tcccagtg-3′), human NOX4 (5′-tctggctctccatgaatgtc-3′, 5′-agaagttgagggcattcacc-3′), human NOX5 (5′-gtgcatcatggaagtcaacc-3′, 5′-ccaaaagtatctcagagccc-3′), or rat NOX1 (5′-cctgctcattttgcaaccac-3′, 5′-catgaga accaaagccacag-3′), rat NOX2 (5′-gacagacttcggaca gtttg-3′, 5′-actctagcttggatacctgg-3′) and rat NOX4 (5′-gtgtttgagcagagcttctg-3′, 5′-gtgaagagaagctttctggg-3′). Purified PCR fragments were subcloned in pCR2.1 TOPO (Invitrogen) and validated by sequencing (GENterprise Gesellschaft für Genanalyse und Biotechnologie mbH, Mainz, Germany).

Cell culture

A7r5 cells (rat, smooth muscle embryonic aorta, ATCC-No. CRL 1444) were cultured in Dulbecco's modified Eagle's medium (Sigma, Deisenhofen, Germany) supplemented with 0.1% glucose, 10% heat-inactivated calf serum, 100 U·mL^{-1} penicillin, 100 µg·mL^{-1} streptomycin and 2 mM glutamine. CaCo-2 cells (human, adenocarcinoma, colon, ATCC-No. HTB 37) were cultured with medium of the same composition as for A7r5 cells, but additionally supplemented with 1% non-essential amino acids. Cells were cultured at 37°C under an atmosphere of 6% CO_2 until they reached 70–80% confluence. Cells were washed with phosphate-buffered saline (PBS) buffer (2.7 mM KCl, 1.5 mM KH_2PO_4, 137 mM NaCl, 8 mM Na_2HPO_4, pH 7.3) and detached using a solution of trypsin (0.05%) and EDTA (0.02%) in PBS buffer. Subsequently, cells were counted and resuspended in reaction buffer [140 mM NaCl, 5 mM KCl, 0.8 mM $MgCl_2 \times 2H_2O$, 1.8 mM $CaCl_2 \times 2H_2O$, 1 mM Na_2HPO_4, 25 mM HEPES, 0,1% (w/v) glucose, complete EDTA-free protease inhibitor cocktail; pH 7.3] to a concentration of 2×10^6 cells·mL^{-1}.

HL-60 cells (human, promyeloblast, ATCC-No. CCL 240) were cultured in RPMI-1640 medium (PAA Laboratories GmbH, Pasching, Austria) supplemented with 5% fetal calf serum, penicillin (100 U·mL^{-1}), streptomycin (100 µg·mL^{-1}) and glutamine (2 mM). Cell suspensions (5×10^5 cells·mL^{-1}) were incubated with 1.25% DMSO for 6 days to induce differentiation into granulocyte-like cells. Differentiated cells were centrifuged at 300× *g*, washed with Hanks's balanced salt solution (HBSS, PAA Laboratories GmbH) and resuspended in HBSS to a final concentration of 4.4×10^6 cells·mL^{-1}.

NADPH oxidase activity assay in cell homogenates

In CaCo-2 and A7r5 whole-cell homogenates (WCHs), NADPH oxidase-catalysed ROS formation was measured using lucigenin-enhanced chemiluminescence according to the protocol of Li and Shah (2001) with slight modifications. A7r5 and CaCo-2 cells were suspended in reaction buffer (2×10^6 cells·mL^{-1}) and then underwent three freeze (–20°C) thaw cycles to produce WCH. We routinely confirmed complete lysis of the cells under the microscope. The chemiluminescent probe lucigenin was added to WCH to a final concentration of 5 µM. Then, 100 µL aliquots of WCH (2×10^5 cells equivalent) were transferred to individual wells of an opaque white 96-well plate. Inhibitors were directly added to the wells in the specified concentrations, and the reaction mixture was incubated for 30 min at 37°C in the dark. Subsequently, the reaction was started by the addition of 100 µM NADPH, and chemiluminescence was recorded every 3 min over a period of 9 min (CaCo-2) or 21 min (A7r5) in a luminescence reader (Fluoroscan Ascent FL; Thermo Labsystems, Vantaa, Finland). All measurements were performed in duplicate and repeated at least three times. Results are expressed as area under the curve (AUC), normalized as either a percentage of the NADPH-induced signal in untreated WCH or as a percentage of the superoxide dismutase (SOD) (250 U·mL^{-1})/catalase (CAT) (1000 U·mL^{-1}) inhibitable control signal.

Whole-cell NADPH oxidase activity assay

During the oxidative burst stimulated by phorbol myristate acetate (PMA) in HL-60 cells, NADPH oxidase activity was measured using the superoxide-specific chemiluminescent probe L012. L012 was added to DMSO-differentiated HL-60 cell suspensions to a final concentration of 100 µM. At this concentration, L012 is reportedly devoid of redox cycling properties (Sohn *et al.*, 1999). Then, 100 µL aliquots of cell suspension (4.4×10^5 cells) were transferred to individual wells of a 96-well plate. Inhibitors were directly added to the wells at the specified concentrations. Following a 30 min incubation at 37°C in the dark, the oxidative burst was initiated by the addition of 100 nM PMA, and the chemiluminescence signal was recorded every 5 min over a period of 60 min in the luminescence reader mentioned above. All measurements were performed in duplicate and repeated at least three

times. Results were expressed as AUC normalized as a percentage of the signal generated by untreated PMA-stimulated HL-60 cells.

A second series of experiments was performed in which we used cytochrome *c* reduction as an alternative measure of superoxide production. Cytochrome *c* was added to the DMSO-differentiated HL-60 cell suspension to a final concentration of 100 μM. Then, 100 μL aliquots (4.4×10^5 cells) were transferred to individual wells of a 96-well plate. Following the direct addition of inhibitors, cells were incubated for 30 min at 37°C in the dark. Subsequently, the oxidative burst was initiated by the addition of PMA (final concentration 100 nM) and the cells incubated for 120 min at 37°C. Absorbance was then measured at 540 nm (isosbestic point of cytochrome *c*) and 550 nm (SpectraMax 340; Molecular Devices, Sunnyvale, CA, USA). Each experiment was performed in duplicate and repeated at least three times. Signals were calculated by normalization of the signals obtained at 540 nm. The blank signal (HBSS buffer, cytochrome *c*, PMA) was subtracted and all values expressed relative to the control signal (cells, cytochrome *c*, PMA).

Additional cytochrome *c* assays were performed using opsonized zymosan (OPZ)-treated HL-60 cells instead of PMA treated. OPZ was prepared from zymosan A from *Saccharomyces cerevisiae* (Vejrazka *et al.*, 2005). Briefly, 5 $mg \cdot mL^{-1}$ zymosan A was incubated with normal human serum for 30 min at 37°C. Finally, zymosan was washed and resuspended in HBSS; 500 $\mu g \cdot mL^{-1}$ OPZ was used for stimulation of oxidative burst.

In situ *tissue ROS assay*

All animal care and experimental procedures complied with the recommendations of the Federation of European Laboratory Animals Science Association, and were approved by the local ethics committee. Rats (SHR and WKY) were bred in the animal facilities of the Rudolf Buchheim Institute, Giessen, and fed standard rodent chow and water *ad libitum*. Thoracic aortas of 12- to 14-month-old SHRs ($n = 6$) and WKY ($n = 6$) were embedded in Tissue Tek O.C.T. Compound (Sakura Finetek, Torrance, CA, USA). Unfixed frozen cross sections (5 μm) were incubated with dihydroethidium (DHE) (5 μM; Invitrogen, Darmstadt, Germany) in a light-protected moist chamber at 37°C for 30 min. Before incubation with DHE, serial sections were treated with either L-NAME (100 μM), pegylated SOD (PEG-SOD) (250 $U \cdot mL^{-1}$), oxypurinol (100 μM) or VAS3947 (10 μM) for 30 min at 37°C. Images were obtained with a DM 6000 B fluorescence microscope (Leica, Wetzlar, Germany) using the same imaging settings for each sample. For semi-quantitative analysis of ROS production, total fluorescence intensity was analysed with the FW4000 software (Leica) using three to six images from three sections per aortic ring for each experimental condition.

Xanthine/XOD activity assay

Xanthine (final concentration: 500 μM) and cytochrome *c* (final concentration: 100 μM) were dissolved in HBSS, and 100 μL aliquots of this solution were transferred to individual wells of a 96-well plate. After addition of the inhibitors, the mixtures were allowed to equilibrate for 20 min. The reaction was started by the addition of 100 μL XOD (final concentration: 20 $mU \cdot mL^{-1}$), and absorbance at 540 and 550 nm was recorded 10 min after the start of the reaction (SpectraMax 340; Molecular Devices). Superoxide production was calculated by normalization of the signals obtained at 540 nm. The blank signal (without xanthine) was subtracted.

A L012-based xanthine/XOD assay was performed with the same substances and concentrations as mentioned above using 100 μM L012 instead of cytochrome *c*. After an equilibration time of 20 min, the reaction was started with XOD (20 $mU \cdot mL^{-1}$), and the chemiluminescence was recorded for 20 min in a Fluoroscan FL microplate reader. Signals were calculated as AUC and related to the xanthine/XOD-derived control signal.

Endothelial NOS (eNOS) activity assay

eNOS activity was determined in homogenates of Sf9 cells (derived from *Spodoptera frugiperda*) transfected with a recombinant baculoviral vector expressing human eNOS (Schmidt *et al.*, 1996; Frey *et al.*, 1999). A colorimetric 96-well microtiter plate assay for the determination of enzymatically formed citrulline was performed according to the method of Knipp and Vasak (2000) with slight modifications. Briefly, 90 μL reaction mixture pH 7.5 (100 mM Tris–HCl, 0.05 μM calmodulin, 1 mM $CaCl_2$, 1 μM flavin adenine dinucleotide, 1 μM flavin mononucleotide, 250 μM CHAPSO, 1 mM L-arginine, 5 μM tetrahydrobiopterin, 1 mM NADPH, 2 mM reduced glutathione) was incubated with the specified concentration of NADPH oxidase inhibitors (or the respective solvents) and 5 μL of eNOS cell homogenate for 60 min at 37°C. The reaction was stopped by the addition of 300 μL colour-developing reagent (COLDER), consisting of one part solution A (80 mM diacetylmonoxime, 2 mM thiosemicarbazide) and three parts solution B [3 M H_3PO_4, 6 M H_2SO_4, 2 mM $NH_4Fe(SO_4)_2$]. The mixture was heated for 15 min at 95°C, cooled to room temperature and centrifuged for 5 min at 16 000× *g*. Then, 300 μL of each

sample was transferred to a 96-well microtiter plate, and the absorption at 540 nm was recorded (SpectraMax 340; Molecular Devices). A citrulline calibration curve was performed by mixing 100 µL of 0, 3.125, 6.25, 12.5, 25, 50, 100, 200 or 400 µM citrulline in 100 mM Tris buffer containing 2 mM reduced glutathione with 300 µL COLDER solution, and subsequently treated as described above. Enzyme activity was calculated using the citrulline calibration curve. The effects of NADPH oxidase inhibitors were expressed as a percentage of the respective control solutions. Signal inhibition by L-NAME (1 mM) demonstrated specificity of the assay for NOS. Standards were measured in duplicate, while all other measurements were performed in triplicate and repeated at least twice.

Data analysis

Data analysis was performed using Prism 4.0 for Macintosh (GraphPad Software, San Diego, CA, USA). IC_{50} values of concentration-dependent inhibition curves were calculated with a non-linear regression analysis using an algorithm for sigmoidal dose–response with variable slopes. Results are expressed as mean ± SEM. Statistical differences between the means were analysed by one-way ANOVA followed by Bonferroni's multiple range test. A value of $P < 0.05$ was considered to be significant.

Materials

N,*N*-dimethyl-9,9–biacridinium dinitrate (lucigenin), cytochrome *c* from horse heart, N^G-nitro-L-arginine methyl ester (L-NAME), oxypurinol, SOD from bovine erythrocytes, CAT from bovine liver, PMA, DPI chloride (dissolved in DMSO; 0.3–10 µM) were purchased from Sigma (Deisenhofen, Germany); 8-amino-5-chloro-7-phenylpyrido[3,4-d]pyridazine-1,4-(2H,3H) dione (L012) from Wako (Osaka, Japan); XOD from cow's milk and complete EDTA-free protease inhibitor cocktail from Roche (Mannheim, Germany); 4′-hydroxy-3′-methoxya cetophenone (apocynin) from Calbiochem (Darmstadt, Germany; in 40% ethanol, 3–1000 µM); AEBSF from Merck (Darmstadt, Germany; in HBSS, 3–1000 µM); 3-benzyl-7-(2-oxazolyl)thio-1,2,3-triazolo[4,5-d]pyrimidine (VAS3947) from Vasopharm GmbH (Würzburg, Germany; in DMSO). Synthesis and analytical data for VAS3947 have been described by Tegtmeier *et al*. (2005). The structure of VAS3947 is shown in Figure 1. Solvent controls were performed for all assays and did not have any significant effect, if not stated otherwise.

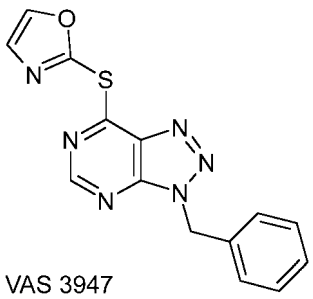

Figure 1

Chemical structure of VAS3947 [3-benzyl-7-(2-oxazolyl)thio-1,2,3-triazolo[4,5-d]pyrimidine]. VAS3947 was characterized by NMR and mass spectrometry [^{1}H nmr (DMSO-D6): δ 5.90 (s, 2H, CH_2), 7.3–7.4 (m, 5H, Ph), 7.6 (s, 1H, Ar), 8.55 (s, 1H, Ar), 8.95 (s, 1H, H-5). ms: (+APCI) *m*/*z* 311 $[M+H]^+$).

Results

CaCo-2, HL-60 and A7r5 cells collectively express all known NOX subunits

First, we wanted to establish cell models that physiologically expressed different NOX isoforms. Therefore, we analysed the NOX mRNA expression patterns using non-quantitative RT-PCR (Figure 2A). In contrast to previous reports, our batch of CaCo-2 cells not only expressed NOX1 mRNA, the predominant isoform in colon (Rokutan *et al*., 2006), but also mRNAs of NOX2, NOX4 and NOX5. As reported, HL-60 cells mainly expressed NOX2 mRNA (Teufelhofer *et al*., 2003), the main isoform in human neutrophils (Babior *et al*., 2002). However, we also detected NOX5 in these cells. Finally, A7r5 cells contained not only NOX4 mRNA, the predominant isoform in VSMCs (Wingler *et al*., 2001), but also NOX3, previously thought to be confined to the inner ear (Banfi *et al*., 2004) and NOX1 (Suh *et al*., 1999). Thus, none of the cell lines was specific for any NOX isoform, and they expressed different NOX isoform patterns. Jointly, the chosen cell lines expressed all NOX isoforms relevant to the cardiovascular system under basal conditions (i.e. NOX1, NOX2, NOX4 and human NOX5).

Cellular ROS formation is independent of XOD and NOS

We next characterized the likely enzymatic source and nature of ROS generated in our chosen cell models. The NADPH-dependent lucigenin (5 µM) chemiluminescence in homogenates represents a frequently used cell-free NADPH oxidase assay. At that low concentration, lucigenin is claimed to be free of relevant redox cycling and artefactual signals (Munzel *et al*., 2002). Using this assay, we found that

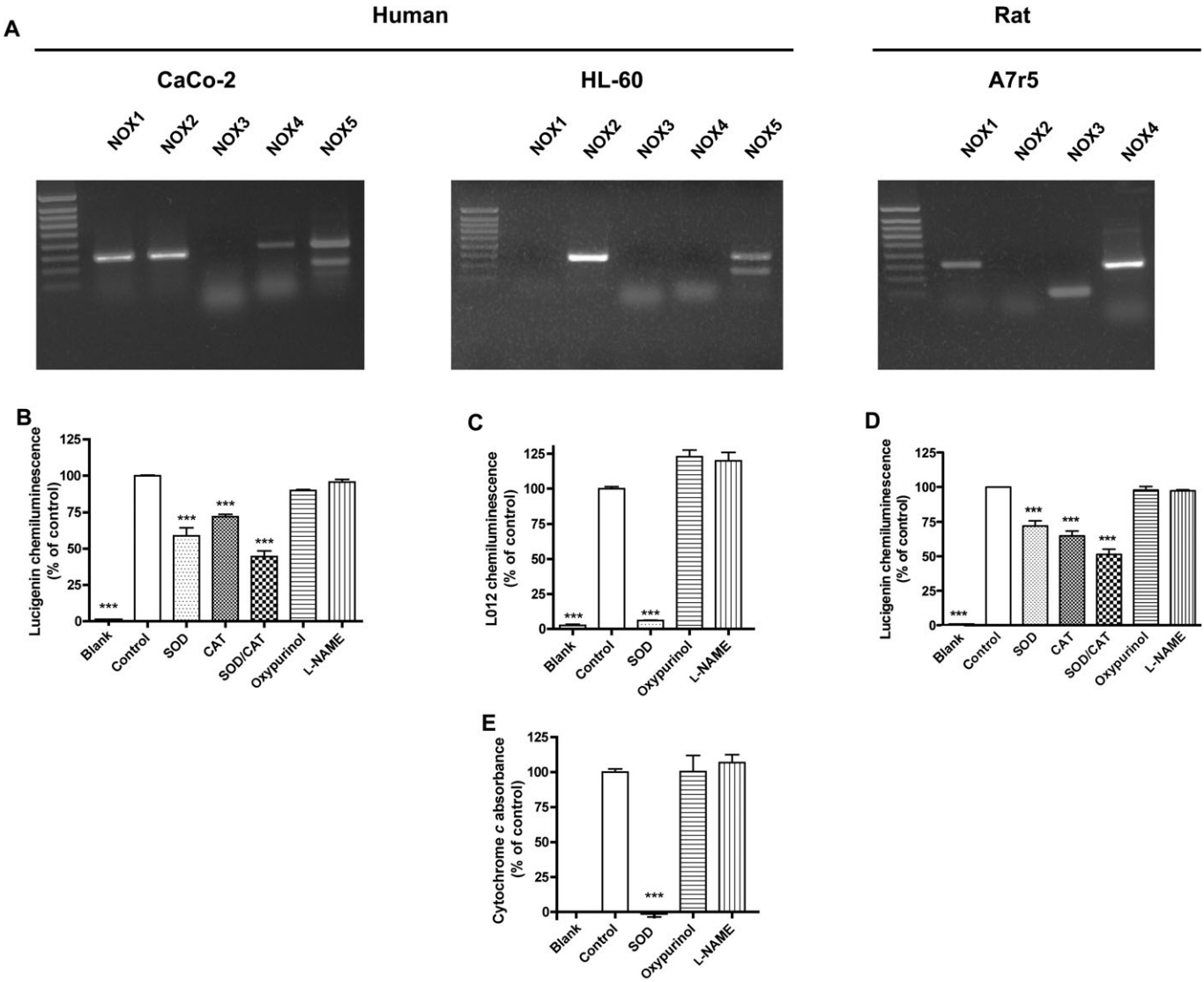

Figure 2

NOX expression and NADPH oxidase activity in three different cell lines. (A) Reverse transcriptase PCR of the five human (NOX1–5) and four rodent (NOX1–4) NOX isoform mRNAs in the human colon epithelial cell line CaCo-2, the human leucoblast cell line HL-60 and the rat aortic smooth muscle cell line A7r5. All cell lines expressed more than one NOX subunit. For measurement of NADPH oxidase activity, CaCo-2 homogenates + substrate NADPH (B), PMA-treated HL-60 cells (C and E) and A7r5 homogenates + substrate NADPH (D) were incubated in the absence or presence of SOD (250 U·mL^{-1}), CAT (1000 U·mL^{-1}), oxypurinol (100 μM) or L-NAME (100 μM). ROS formation was measured by lucigenin (B and D), or L012 (B) chemiluminescence, or by cytochrome *c* reduction (E). In none of the cells, detectable ROS formation originated from NOS (inhibited by L-NAME) or XOD (inhibited by oxypurinol). Only in HL-60 cells, the assay signals were fully inhibited by SOD and thus due to superoxide. In CaCo-2 and A7r5 cell homogenates, even the combination of SOD and CAT only partially attenuated the assay signal, suggesting that only a fraction was due to superoxide and/or H_2O_2. In later experiments, only the SOD/CAT-inhibited signal component was considered as a measure of superoxide/H_2O_2 formation in CaCo-2 and A7r5 cell homogenates. Data labelled 'blank' represent signals in the absence of cells or homogenate. Values represent means ± SEM of $n \geq 6$ observations; ***$P < 0.001$, significantly different from control values.

both SOD and CAT attenuated the signal in CaCo-2 and A7r5 cell homogenates (Figure 2B,D), and we observed an additive effect when combining SOD and CAT. Inhibition of the lucigenin signals by CAT (Rost *et al.*, 1998; Janiszewski *et al.*, 2002), in the absence and presence of SOD, suggested that lucigenin is also sensitive to H_2O_2 (Rost *et al.*, 1998). Both species, superoxide and H_2O_2, may originate from NADPH oxidases (Cai, 2005). Therefore, the SOD/CAT inhibitable fraction of the CaCo-2 and A7r5 signal was utilized as basal ROS formation. Nevertheless, the inhibition by SOD and CAT was not complete. Although we made sure that all cells were lysed, some cell organelles or intracellular vesicles may stay intact under our lysis protocol. NADPH oxidases and ROS can be highly localized, and SOD

and CAT may not enter these organelles, which may explain these observations.

In PMA-stimulated HL-60 cells, the oxidative burst was measured by L012-mediated chemiluminescence (Figure 2C) (Daiber *et al.*, 2004) and cytochrome *c* reduction (Figure 2E). SOD completely abolished the PMA-stimulated signal in both assays, confirming that superoxide is the only detectable ROS released from PMA-stimulated HL-60 cells. Consequently, the entire L012 signal was taken as PMA-stimulated ROS formation in HL-60 cells.

To determine the enzymatic source of ROS, ROS formation was re-assessed in the absence or presence of the NOS inhibitor, L-NAME, and the XOD inhibitor, oxypurinol. Both compounds failed to attenuate the ROS signals in any of the assays, suggesting that neither XOD nor uncoupled NOS are relevant sources of ROS in our cell models under the conditions used.

Antioxidant effects

NOX inhibitors may also reduce ROS signals by direct antioxidant effects (i.e. radical scavenging). Therefore, we performed a xanthine/XOD cytochrome *c* reduction assay, which generates superoxide independent of NADPH oxidase activity. As shown in Figure 3A, DPI and oxypurinol, but none of the other compounds, potently attenuated the XOD signal, suggesting a direct inhibition of XOD. This is consistent with DPI being a flavoprotein inhibitor (Lange *et al.*, 2009) as both NOX and XOD are flavoproteins. Interestingly, when using L012 to detect ROS from xanthine/XOD, apocynin potently interfered with the signal (Figure 3B). This confirms recent reports that apocynin directly scavenges reaction products of H_2O_2, which are detected by L012, but not by cytochrome *c* (Heumuller *et al.*, 2008). Surprisingly, AEBSF increased the L012 signal more than eightfold, suggesting a previously unrecognized interaction between L012 and AEBSF. This may be particularly problematic when AEBSF is used in homogenizing buffers as a serine protease inhibitor (Kobayashi *et al.*, 2007; Baumer *et al.*, 2008). VAS3947 (30 μM) was the only compound that did not interfere with xanthine/XOD-derived L012 signals, suggesting this compound is free of antioxidant or scavenging effects relevant to ROS detection.

Inhibition of non-NOX flavoproteins

In addition to XOD, eNOS was used as a flavoprotein control to test the specificities of NADPH oxidase inhibitors. eNOS, like the catalytic NOX subunit, binds NADPH and contains both a flavin and haem cofactor. As expected, DPI (10 μM) also abolished eNOS activity (Figure 3C), while apocynin (1 mM), AEBSF (1 mM) and VAS3947 (10 μM) had

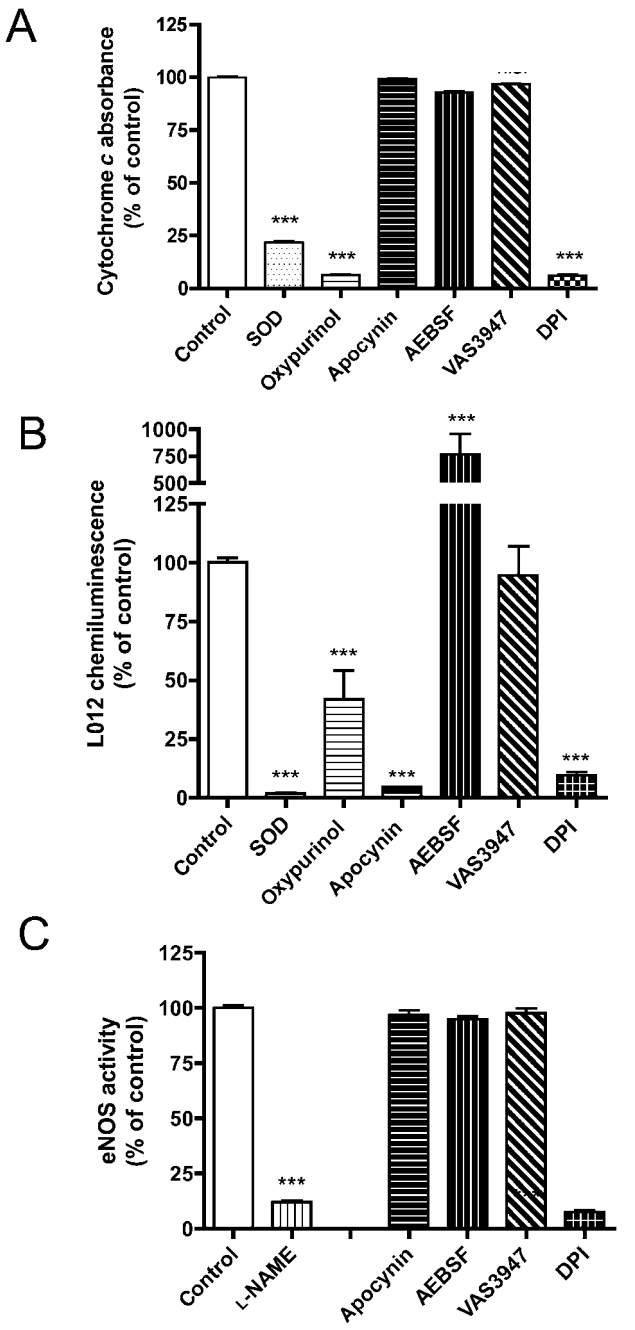

Figure 3

Effect of the NADPH oxidase inhibitors apocynin (1 mM), AEBSF (1 mM), DPI (10 μM) and VAS3947 on the activity of the flavoprotein XOD (30 μM VAS3947), and the flavo-haem protein, eNOS (10 μM VAS3947). XOD activity was assayed by cytochrome *c* reduction (A) or L012 chemiluminescence (B); eNOS activity was determined by L-arginine to L-citrulline conversion using recombinantly expressed eNOS (C). SOD (250 U·mL^{-1}) and oxypurinol (1 mM) served as positive controls for XOD activity and L-NAME (1 mM) for eNOS activity. While apocynin did not scavenge superoxide in the cytochrome *c* reduction assay, it interfered with the L012 chemiluminescence assay. DPI inhibited both XOD and eNOS, and was thus no longer considered for NADPH oxidase enzyme assays in the present study. Values represent means ± SEM of $n \geq 5$ experiments. ***$P < 0.001$, significantly different from control values.

no effect. As DPI inhibited both XOD and eNOS activity in concentrations similar to those needed for NADPH oxidase inhibition, it was no longer considered for further NADPH oxidase enzyme assays in the present study. We also tested higher concentrations (up to 100 μM) of VAS3947, and neither found an effect on XOD nor on eNOS activity (not shown).

Concentration dependence and efficacy

We next investigated the concentration dependence and efficacy of the remaining compounds, apocynin, AEBSF and VAS3947. In CaCo-2 cell homogenates, VAS3947 completely blocked NADPH-dependent ROS production with an IC_{50} of 12 μM, whereas apocynin and AEBSF caused only modest inhibition (Figure 4A). In contrast, the L012 chemiluminescence signal from HL-60 cells was inhibited by all three compounds (Figure 4B). The IC_{50} values for apocynin and VAS3947 were 97 and 2 μM respectively. Surprisingly, AEBSF exerted a biphasic response with concentrations <300 μM increasing the signal (EC_{50} = 30 μM) and higher concentrations being inhibitory (IC_{50} = 0.42 mM). Considering the increased signal in the L012 xanthine/XOD assay in the presence of AEBSF (Figure 3B), a direct interaction between AEBSF and L012 is likely. Because apocynin exerted non-specific effects in the L012 xanthine/XOD assay, we hypothesized that the inhibition seen in this HL-60 cell assay may not necessarily be due to inhibition of NADPH oxidases. Indeed, when using cytochrome *c* as a detection reagent in HL-60 cells (Figure 4B), apocynin had only a minor effect, while VAS3947 still completely inhibited with a similar IC_{50} value (1 μM) as observed in the L012 assay. In contrast to the L012 assay, AEBSF inhibited the cytochrome *c* reduction signal in a monophasic manner and had a high IC_{50} value of 0.3 mM similar to the second inhibitory phase with L012 (0.42 mM; see above).

We hypothesized that apocynin was insufficiently metabolized by PMA-stimulated HL-60 cells and thus did not inhibit cytochrome *c* reduction mediated by these cells. Previous observations suggest that apocynin may be a pro-drug requiring activation by myeloperoxidases (Heumuller *et al.*, 2008). Therefore, HL-60 cells were stimulated with OPZ, which, in contrast to PMA, activates not only NADPH oxidases, but also myeloperoxidase. Indeed, under these conditions, apocynin attenuated cytochrome *c* reduction (data not shown). VAS3947 and AEBSF were as effective in OPZ as in PMA-treated HL-60 cells (data not shown). In summary, VAS3947 was the only compound to effectively and consistently inhibit the oxidative burst signal in HL-60 cells independent of the stimulus and the read-out reagent.

Results obtained with homogenates of the third cell line, A7r5, were similar to those obtained with CaCo-2 cell homogenates when using the same lucigenin assay. Apocynin and AEBSF partially, and VAS3947 fully attenuated the NADPH-stimulated signal (Figure 4D). The IC_{50} values calculated from the concentration–response curves suggested millimolar potency for apocynin (1.9 mM) and AEBSF (1.2 mM), and micromolar potency for VAS3947 (13 μM). Thus, VAS3947 also inhibits NADPH oxidase in a vascular cell line mainly expressing NOX4 and NOX3, whereas apocynin and AEBSF were only weak inhibitors in this model with IC_{50} values approximately 100 times that for VAS3947.

NADPH oxidases are the main source of ROS in the SHR aorta

Having established that apocynin and AEBSF have considerably different IC_{50} values and are ineffective in some NOX model systems, whereas VAS3947 consistently inhibited NADPH oxidase activity in all three cell lines with similar IC_{50} values, we considered VAS3947 as the most reliable NADPH inhibitor. VAS3947 was therefore used as a pharmacological tool to investigate the source of ROS in aortas of aged SHRs (Figure 5), an established model of hypertension and cardiovascular oxidative stress. The *in situ* DHE stain is not specific for any ROS and rather summarizes superoxide-, peroxide- and peroxynitrite-mediated oxidative chemistry. This DHE stain of SHR aortas was significantly higher throughout the aortic wall compared to the signal in aortas from WKY control rats. Furthermore, it was blocked by PEG-SOD and was resistant to both L-NAME and oxypurinol. This suggested that superoxide was a major product leading to DHE oxidation, and that it was neither derived from eNOS nor XOD. Importantly, VAS3947 effectively inhibited DHE-detectable ROS formation in SHR aortas, suggesting that NADPH oxidases are a relevant enzymatic source of ROS throughout the aortic wall of aged SHRs.

Discussion

In the present study, we established the comparative pharmacology of the most frequently used and novel NADPH oxidase inhibitors, applying some of the most commonly used ROS assays. Of all inhibitors investigated, the novel triazolo pyrimidine, VAS3947, was the only compound that neither interfered with the flavoprotein, XOD, or the flavohaem protein, eNOS, had no significant antioxidant activity, nor interfered with any of the ROS detection assays. Rather, VAS3947 effectively inhibited

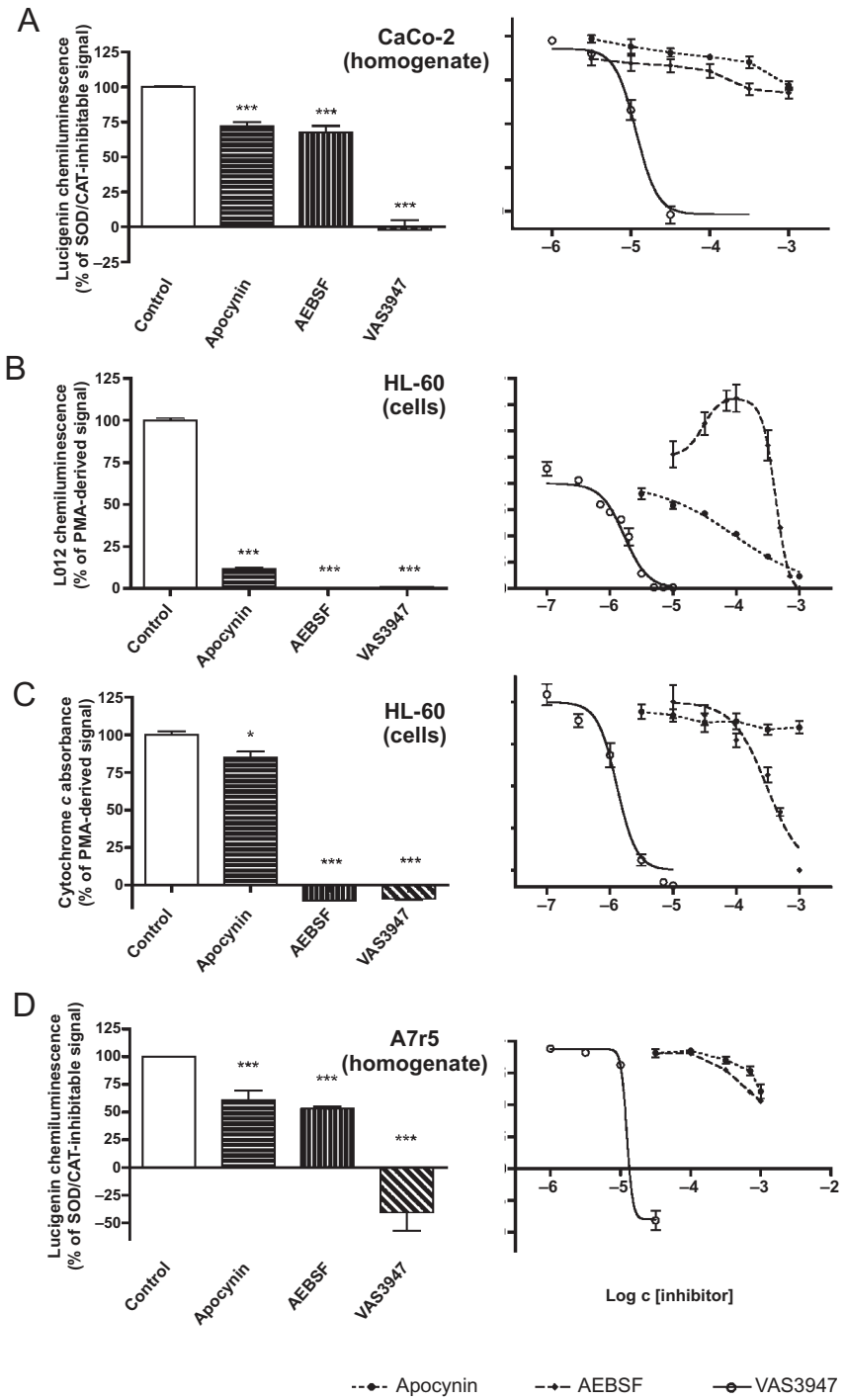

Figure 4

Maximal inhibition and potency of apocynin, AEBSF and VAS3947 to inhibit NADPH oxidase activity. Activity was measured in CaCo-2 (A) or A7r5 (D) cell homogenates as NADPH-induced and SOD/CAT-inhibitable lucigenin-derived chemiluminescence, or in DMSO-differentiated HL-60 cells as measured by L012-derived chemiluminescence (B) or cytochrome *c* reduction (C). The left panels depict maximal inhibition; the right panels concentration–response curves. Concentrations used for maximal inhibition were in CaCo-2 cell homogenates 1 mM apocynin, 1 mM AEBSF and 30 μM VAS3947 (A); in HL-60 cell-mediated L012 chemiluminescence 1 mM apocynin, 100 μM AEBSF and 10 μM VAS3947 (B); in HL-60 cell-mediated cytochrome *c* reduction 1 mM apocynin, 1 mM AEBSF and 10 μM VAS3947 (C); and in A7r5 cell homogenates 1 mM apocynin, 1 mM AEBSF and 30 μM VAS3947 (D). IC_{50} values for VAS3947 were 12 μM (A), 2 μM (B), 1 μM (C) and 13 μM (D). Apocynin had a potency in the micromolar range (97 μM) only in the HL-60/L012 assay (B). AEBSF had the lowest potency (420 μM in B, 304 μM in C; 1.2 mM in D), and in the HL-60/L012 assay it even enhanced signal intensity at low micromolar concentrations (EC_{50} = 30 μM). Values represent means ± SEM of $n \geq 5$ experiments. *$P < 0.05$, ***$P < 0.001$, significantly different from control values.

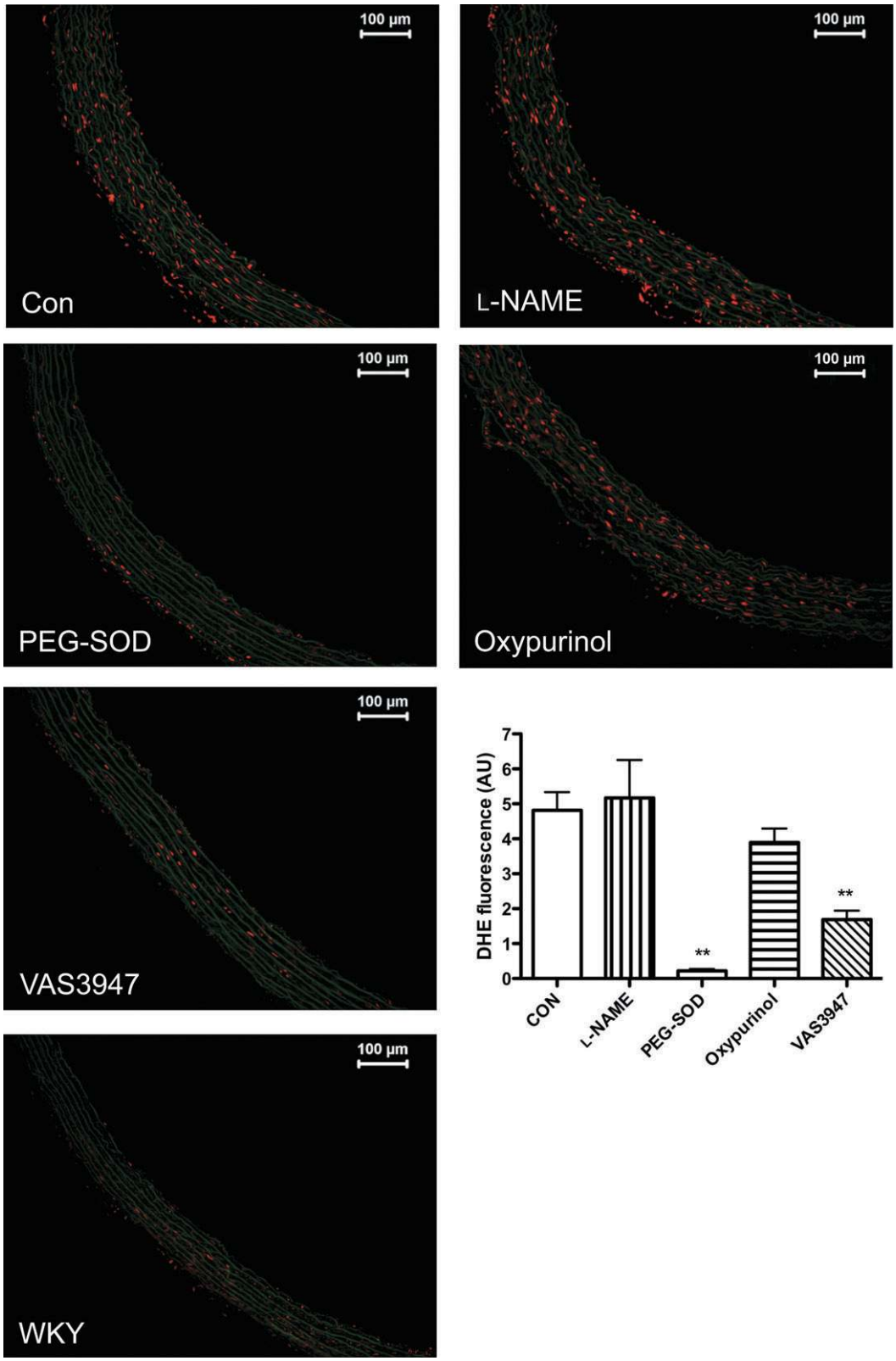

Figure 5

Effect of the NADPH oxidase inhibitors on ROS formation in aortic sections from 12- to 14-month-old SHRs as determined by *in situ* DHE tissue stain. DHE signals are enhanced in SHR versus WKY rat aorta, and correlate with enhanced levels of NOX1, 2 and 4. Sections were incubated either in the absence (Con) or presence of L-NAME (100 µM), PEG-SOD (250 $U \cdot mL^{-1}$), oxypurinol (100 µM) or VAS3947 (10 µM). Signal intensity was quantified and expressed as mean ± SEM of three experiments ($n = 6$). $^{**}P < 0.01$, significantly different from control (CON).

NADPH oxidase activity in three cellular models expressing different patterns of all known NOX isoforms. Therefore, at least *in vitro*, triazolo pyrimidines are new pharmacological tools for inhibiting NADPH oxidases. Applying this novel tool, we were able to establish that NADPH oxidases are a major source of ROS in aortas of aged hypertensive rats.

Based on genetic and other data, NADPH oxidases potentially play a major role in the development and progression of cardiovascular diseases (Williams and Griendling, 2007). This would suggest that it might be beneficial to therapeutically target NADPH oxidases. Apart from genetic mouse models, pharmacological agents are essential to provide proof-of-principle in non-mouse species and to serve as experimental therapeutics. The first triazolo pyrimidine described as an NADPH oxidase inhibitor was VAS2870, stemming from a systematic compound screen in HL-60 cells. VAS2870 inhibits NADPH oxidase activity in oxLDL-exposed HUVEC (Stielow *et al.*, 2006) and PDGF-stimulated primary rat aortic VSMC (ten Freyhaus *et al.*, 2006). VAS2870 also inhibits the stimulation of vasculogenesis of mouse embryonic stem cells upon treatment with PDGF-BB (Lange *et al.*, 2009), and it inhibits wound margin H_2O_2 production without obvious toxicity in zebrafish larvae (Niethammer *et al.*, 2009). In addition, VAS2870 does not interact with ROS in an antioxidant manner nor does it interfere with XOD (ten Freyhaus *et al.*, 2006). However, a major disadvantage of VAS2870 is its poor solubility. Therefore, a closely related derivative, VAS3947, was developed with an approximately four times better solubility (data not shown). Apart from the solubility, VAS3947 has strikingly similar properties compared to VAS2870. For example, the IC_{50} values for NADPH oxidase activity of PMA-stimulated HL-60 cells, PMA-stimulated whole blood and freshly isolated human lymphocytes stimulated with PMA are essentially the same for both compounds (unpublished data). VAS3947 (this study) and VAS2870 (not shown) both effectively inhibit ROS production in aortas of SHRs as assessed by *in situ* DHE staining. Taken together, our evidence shows that: (i) the potential to inhibit NADPH oxidases is a class effect of triazolo pyrimidines; and (ii) this compound class inhibits NADPH oxidase activity in a variety of cell types and tissues of phagocytic, as well as non-phagocytic, origin with similar efficacy.

Our emphasis was to characterize the compounds in the most commonly used assays. We have therefore used alternative ways to characterize NADPH oxidase inhibitors: PMA-stimulated ROS release from HL-60 cells and NADPH-stimulated ROS production in cell homogenates. For detection, we used cytochrome *c*, L012 and lucigenin. We are aware that these assays do have drawbacks. Lucigenin-enhanced chemiluminescence has been widely used and is reported to be reasonably specific for superoxide. The lack of complete inhibition of the lucigenin signal by SOD that we observed was also reported by others (Rost *et al.*, 1998). This indicates that it is not completely specific for superoxide. Lucigenin can penetrate cells and is prone to redox cycling. However, when 5 μM is used, the amount of artefact is probably insignificant (Dikalov *et al.*, 2007). Compared to lucigenin, L012 is more sensitive for the detection of ROS (Daiber *et al.*, 2004). H_2O_2 does not significantly contribute to L012-enhanced chemiluminescence. However, in addition to reacting with superoxide, L012 also detects peroxynitrite (Daiber *et al.*, 2004). In contrast to lucigenin, L012 only detects extracellular ROS, as does cytochrome *c*, which considered as a 'gold standard' for detection of superoxide released in large amounts, such as during the respiratory burst of neutrophils. A disadvantage is its poor sensitivity (Dikalov *et al.*, 2007).

In comparison to VAS3947, DPI is a less suitable pharmacological tool to validate the involvement of NADPH oxidase because of its effects on other flavoenzymes, such as XOD and eNOS, as well as on cholinesterases and the internal calcium pump (Tazzeo *et al.*, 2009). In our hands, apocynin had only minor efficacy and potency. This may in part be due to the fact that apocynin is a pro-drug requiring metabolic activation by myeloperoxidases. Furthermore, in PMA-stimulated HL-60 cells, the inhibition of the L012 signal by apocynin was caused by interference with the assay, either due to antioxidative effects or a direct interaction with L012. Thus, inhibitory effects of apocynin in the L012 assay may not necessarily reflect inhibition of NADPH oxidase activity (Heumuller *et al.*, 2008). Interestingly, upon oxidation of apocynin during its activation, the resulting apocynin radical becomes a potent pro-oxidant with high capacity to oxidize thiols and NADPH. The depletion of NADPH potentially reduces NADPH oxidase activity (Castor *et al.*, 2010). AEBSF was a similarly weak NADPH oxidase inhibitor in CaCo-2 and A7r5 cell homogenates, possibly indicating an only minor role for p47phox-dependent NADPH oxidases in these cells. Indeed, NOXO1 and/or NOXA1, homologues of p47phox and p67phox, may be of more relevance in CaCo-2 cells and not affected by AEBSF (Banfi *et al.*, 2003; Takeya *et al.*, 2003). In NADPH-stimulated homogenates from A7r5 cells, NOX4 may be the main source of ROS and independent of cytosolic subunits. While AEBSF attenuated the oxidative burst of HL-60 cells at high concentrations in the L012 and

the cytochrome *c* assay, it may not be advisable to use this compound as an NADPH oxidase inhibitor because it obviously interferes with L012 and has off-target effects such as serine protease inhibition (Diatchuk *et al.*, 1997).

The mechanism of action of triazolo pyrimidines such as VAS3947 and VAS2870 is unclear. In human leucocytes, VAS2870 does not inhibit translocation of p47phox to the membrane (ten Freyhaus *et al.*, 2006), but may still interfere with oxidase assembly once the translocation has occurred. This assumption is supported by experiments showing that VAS2870 inhibits NOX2 activity in a cell-free system when added before (ten Freyhaus *et al.*, 2006), but not after complex formation and stimulation of the oxidase (unpublished observations). The consistent potency and efficacy of VAS3947 in different cell and tissue models indicate that VAS3947, in contrast to apocynin, is not a pro-drug.

VAS3947 effectively suppressed the DHE signal in aortas of aged SHRs, suggesting that NADPH oxidases are indeed a major source of ROS in this disease model and that these enzymes can be pharmacologically targeted. However, the pharmacokinetic profile of VAS3947 and the *in vivo* efficacy, as well as long-term effects of NADPH oxidase inhibition, are unknown. In this context, peptide-based NADPH oxidase inhibitors are more advanced. The NOX2 homologous fusion peptide, gp91ds-tat (Rey *et al.*, 2001), which interferes with cytosolic subunit translocation and activation of NOX2, inhibits angiotensin II-induced aortic superoxide production and hypertension *in vivo* (Rey *et al.*, 2001). In addition, adenoviral expression of this peptide sequence in blood vessel adventitia had a beneficial effect, preventing neointimal hyperplasia (Dourron *et al.*, 2005). Because our focus was on small synthetic molecules, and not on peptides, we did not include gp91ds-tat in our study. Nevertheless, NOX1-, NOX3-, NOX4- and NOX5-specific tat-peptide analogues may become useful pharmacological tools in the future.

In conclusion, apocynin, AEBSF and DPI appear to lack specificity as pharmacological agents when validating the involvement of NADPH oxidases in any physiological or pathological function. In contrast, triazolo pyrimidines such as VAS3947 are specific for NADPH oxidases versus NOS and XOD, and do not interfere with commonly used ROS assay systems. However, we cannot exclude the possibility that VAS3947, in addition to inhibiting NADPH oxidases, also interferes with alternative sources of ROS that we have not yet investigated, such as the mitochondrial electron chain. Future studies will be required to clarify the precise mechanism of action and *in vivo* efficacy of triazolo pyrimidines, and – once several derivatives become available – their isoform selectivity. For *in vivo* experiments, derivatives with higher solubility are essential. Importantly, by applying VAS3947 to the SHR model, we here have provided validated pharmacological evidence that NADPH oxidases are a relevant source of ROS in hypertension.

Acknowledgements

This work was funded by grants from the Deutsche Forschungsgemeinschaft, SFB547/C7 (H.H.H.W.S.), the Bayerische Forschungsstiftung (K.W. and H.H.H.W.S.) and the National Health and Medical Research Council of Australia (H.H.H.W.S.).

Conflict of interest

H.H.H.W.S. declares that he holds shares in Vasopharm GmbH, which develops NADPH oxidase inhibitors pharmaceutically. H.H.H.W.S., K.W. and P.S. are inventors of a patent on VAS3947, which is owned by Vasopharm GmbH. P.S. is employed by Vasopharm GmbH. K.W. is a former employee of Vasopharm GmbH.

References

Babior BM, Lambeth JD, Nauseef W (2002). The neutrophil NADPH oxidase. Arch Biochem Biophys 397: 342–344.

Banfi B, Clark RA, Steger K, Krause KH (2003). Two novel proteins activate superoxide generation by the NADPH oxidase NOX1. J Biol Chem 278: 3510–3513.

Banfi B, Malgrange B, Knisz J, Steger K, Dubois-Dauphin M, Krause KH (2004). NOX3, a superoxide-generating NADPH oxidase of the inner ear. J Biol Chem 279: 46065–46072.

Baumer AT, Ten Freyhaus H, Sauer H, Wartenberg M, Kappert K, Schnabel P *et al.* (2008). Phosphatidylinositol 3-kinase-dependent membrane recruitment of Rac-1 and p47phox is critical for alpha-platelet-derived growth factor receptor-induced production of reactive oxygen species. J Biol Chem 283: 7864–7876.

Bayraktutan U (2005). Coronary microvascular endothelial cell growth regulates expression of the gene encoding p22-phox. Free Radic Biol Med 39: 1342–1352.

Bedard K, Krause KH (2007). The NOX family of ROS-generating NADPH oxidases: physiology and pathophysiology. Physiol Rev 87: 245–313.

Brandes RP, Kreuzer J (2005). Vascular NADPH oxidases: molecular mechanisms of activation. Cardiovasc Res 65: 16–27.

Cai H (2005). NAD(P)H oxidase-dependent self-propagation of hydrogen peroxide and vascular disease. Circ Res 96: 818–822.

Castor LR, Locatelli KA, Ximenes VF (2010). Pro-oxidant activity of apocynin radical. Free Radic Biol Med 48: 1636–1643.

Cave AC, Brewer AC, Narayanapanicker A, Ray R, Grieve DJ, Walker S *et al.* (2006). NADPH oxidases in cardiovascular health and disease. Antioxid Redox Signal 8: 691–728.

Daiber A, August M, Baldus S, Wendt M, Oelze M, Sydow K *et al.* (2004). Measurement of NAD(P)H oxidase-derived superoxide with the luminol analogue L-012. Free Radic Biol Med 36: 101–111.

Diatchuk V, Lotan O, Koshkin V, Wikstroem P, Pick E (1997). Inhibition of NADPH oxidase activation by 4-(2-aminoethyl)-benzenesulfonyl fluoride and related compounds. J Biol Chem 272: 13292–13301.

Dikalov S, Griendling KK, Harrison DG (2007). Measurement of reactive oxygen species in cardiovascular studies. Hypertension 49: 717–727.

Dourron HM, Jacobson GM, Park JL, Liu J, Reddy DJ, Scheel ML *et al.* (2005). Perivascular gene transfer of NADPH oxidase inhibitor suppresses angioplasty-induced neointimal proliferation of rat carotid artery. Am J Physiol Heart Circ Physiol 288: H946–H953.

Frey A, Schneider-Rasp S, Marienfeld U, Yu JC, Paul M, Poller W *et al.* (1999). Biochemical and functional characterization of nitric oxide synthase III gene transfer using a replication-deficient adenoviral vector. Biochem Pharmacol 58: 1155–1166.

ten Freyhaus H, Huntgeburth M, Wingler K, Schnitker J, Baumer AT, Vantler M *et al.* (2006). Novel Nox inhibitor VAS2870 attenuates PDGF-dependent smooth muscle cell chemotaxis, but not proliferation. Cardiovasc Res 71: 331–341.

Gavazzi G, Banfi B, Deffert C, Fiette L, Schappi M, Herrmann F *et al.* (2006). Decreased blood pressure in NOX1-deficient mice. FEBS Lett 580: 497–504.

Griendling KK, Sorescu D, Ushio-Fukai M (2000). NAD(P)H oxidase: role in cardiovascular biology and disease. Circ Res 86: 494–501.

Heumuller S, Wind S, Barbosa-Sicard E, Schmidt HH, Busse R, Schroder K *et al.* (2008). Apocynin is not an inhibitor of vascular NADPH oxidases but an antioxidant. Hypertension 51: 211–217.

Janiszewski M, Souza HP, Liu X, Pedro MA, Zweier JL, Laurindo FR (2002). Overestimation of NADH-driven vascular oxidase activity due to lucigenin artifacts. Free Radic Biol Med 32: 446–453.

Knipp M, Vasak M (2000). A colorimetric 96-well microtiter plate assay for the determination of enzymatically formed citrulline. Anal Biochem 286: 257–264.

Kobayashi M, Ohura I, Kawakita K, Yokota N, Fujiwara M, Shimamoto K *et al.* (2007). Calcium-dependent protein kinases regulate the production of reactive oxygen species by potato NADPH oxidase. Plant Cell 19: 1065–1080.

Lambeth JD, Kawahara T, Diebold B (2007). Regulation of Nox and Duox enzymatic activity and expression. Free Radic Biol Med 43: 319–331.

Lange S, Heger J, Euler G, Wartenberg M, Piper HM, Sauer H (2009). Platelet-derived growth factor BB stimulates vasculogenesis of embryonic stem cell-derived endothelial cells by calcium-mediated generation of reactive oxygen species. Cardiovasc Res 81: 159–168.

Lassegue B, Clempus RE (2003). Vascular NAD(P)H oxidases: specific features, expression, and regulation. Am J Physiol Regul Integr Comp Physiol 285: R277–R297.

Lee MY, Martin AS, Mehta PK, Dikalova AE, Garrido AM, Datla SR *et al.* (2009). Mechanisms of vascular smooth muscle NADPH oxidase 1 (Nox1) contribution to injury-induced neointimal formation. Arterioscler Thromb Vasc Biol 29: 480–487.

Li JM, Shah AM (2001). Differential NADPH- versus NADH-dependent superoxide production by phagocyte-type endothelial cell NADPH oxidase. Cardiovasc Res 52: 477–486.

McNally JS, Davis ME, Giddens DP, Saha A, Hwang J, Dikalov S *et al.* (2003). Role of xanthine oxidoreductase and NAD(P)H oxidase in endothelial superoxide production in response to oscillatory shear stress. Am J Physiol Heart Circ Physiol 285: H2290–H2297.

Matsuno K, Yamada H, Iwata K, Jin D, Katsuyama M, Matsuki M *et al.* (2005). Nox1 is involved in angiotensin II-mediated hypertension: a study in Nox1-deficient mice. Circulation 112: 2677–2685.

Munzel T, Afanas'ev IB, Kleschyov AL, Harrison DG (2002). Detection of superoxide in vascular tissue. Arterioscler Thromb Vasc Biol 22: 1761–1768.

Niethammer P, Grabher C, Look AT, Mitchison TJ (2009). A tissue-scale gradient of hydrogen peroxide mediates rapid wound detection in zebrafish. Nature 459: 996–999.

O'Donnell BV, Tew DG, Jones OT, England PJ (1993). Studies on the inhibitory mechanism of iodonium compounds with special reference to neutrophil NADPH oxidase. Biochem J 290 (Pt 1): 41–49.

Opitz N, Drummond GR, Selemidis S, Meurer S, Schmidt HH (2007). The 'A's and 'O's of NADPH oxidase regulation: a commentary on 'Subcellular Localization and Function of Alternatively Spliced Noxo1 Isoforms'. Free Radic Biol Med 42: 175–179.

Rey FE, Cifuentes ME, Kiarash A, Quinn MT, Pagano PJ (2001). Novel competitive inhibitor of NAD(P)H oxidase assembly attenuates vascular O(2)(–) and systolic blood pressure in mice. Circ Res 89: 408–414.

Rokutan K, Kawahara T, Kuwano Y, Tominaga K, Sekiyama A, Teshima-Kondo S (2006). NADPH oxidases in the gastrointestinal tract: a potential role of Nox1 in innate immune response and carcinogenesis. Antioxid Redox Signal 8: 1573–1582.

Rost M, Karge E, Klinger W (1998). What do we measure with luminol-, lucigenin- and penicillin-amplified chemiluminescence? 1. Investigations with hydrogen peroxide and sodium hypochlorite. J Biolumin Chemilumin 13: 355–363.

Schluter T, Steinbach AC, Steffen A, Rettig R, Grisk O (2008). Apocynin-induced vasodilation involves Rho kinase inhibition but not NADPH oxidase inhibition. Cardiovasc Res 80: 271–279.

Schmidt HH, Hofmann H, Schindler U, Shutenko ZS, Cunningham DD, Feelisch M (1996). No NO from NO synthase. Proc Natl Acad Sci U S A 93: 14492–14497.

Sohn HY, Gloe T, Keller M, Schoenafinger K, Pohl U (1999). Sensitive superoxide detection in vascular cells by the new chemiluminescence dye L-012. J Vasc Res 36: 456–464.

Stielow C, Catar RA, Muller G, Wingler K, Scheurer P, Schmidt HH *et al*. (2006). Novel Nox inhibitor of oxLDL-induced reactive oxygen species formation in human endothelial cells. Biochem Biophys Res Commun 344: 200–205.

Stocker R, Keaney JF, Jr (2004). Role of oxidative modifications in atherosclerosis. Physiol Rev 84: 1381–1478.

Suh YA, Arnold RS, Lassegue B, Shi J, Xu X, Sorescu D *et al*. (1999). Cell transformation by the superoxide-generating oxidase Mox1. Nature 401: 79–82.

Takeya R, Ueno N, Kami K, Taura M, Kohjima M, Izaki T *et al*. (2003). Novel human homologues of p47phox and p67phox participate in activation of superoxide-producing NADPH oxidases. J Biol Chem 278: 25234–25246.

Tazzeo T, Worek F, Janssen L (2009). The NADPH oxidase inhibitor diphenyleneiodonium is also a potent inhibitor of cholinesterases and the internal Ca(2+) pump. Br J Pharmacol 158: 790–796.

Tegtmeier F, Walter U, Schinzel R, Wingler K, Scheurer P, Schmidt H (2005). Compounds containing a *N*-heteroaryl moiety linked to fused ring moieties for the inhibition of NAD(P)H oxidases and platelet activation. European Patent 1 598 354 A1.

Teufelhofer O, Weiss R-M, Parzefall W, Schulte-Hermann R, Micksche M, Berger W *et al*. (2003). Promyelocytic HL60 cells express NADPH oxidase and are excellent targets in a rapid spectrophotometric microplate assay for extracellular superoxide. Toxicol Sci 76: 376–383.

Vejrazka M, Micek R, Stipek S (2005). Apocynin inhibits NADPH oxidase in phagocytes but stimulates ROS production in non-phagocytic cells. Biochim Biophys Acta 1722: 143–147.

Williams HC, Griendling KK (2007). NADPH oxidase inhibitors: new antihypertensive agents? J Cardiovasc Pharmacol 50: 9–16.

Wingler K, Wunsch S, Kreutz R, Rothermund L, Paul M, Schmidt HH (2001). Upregulation of the vascular NAD(P)H-oxidase isoforms Nox1 and Nox4 by the renin-angiotensin system *in vitro* and *in vivo*. Free Radic Biol Med 31: 1456–1464.